



Characterization of Electrodeposited Technetium on Gold Foil

Edward Mausolf,² Frederic Poineau, Thomas Hartmann,
Janelle Droessler, and Ken Czerwinski

Radiochemistry Program, Department of Chemistry, University of Nevada, Las Vegas, Las Vegas,
Nevada 89154, USA

The reduction and electrodeposition of TcO_4^- on a smooth gold foil electrode with an exposed area of 0.25 cm^2 was performed in $1 \text{ M H}_2\text{SO}_4$ supporting electrolyte using bulk electrolysis with a constant current density of 1.0 A/cm^2 at a potential of -2.0 V . Significant hydrogen evolution accompanied the formation of Tc deposits. Tc concentrations consisted of 0.01 M and $2 \times 10^{-3} \text{ M}$ and were electrodeposited over various times. Deposited fractions of Tc were characterized by powder x-ray diffraction, x-ray absorption fine structure spectroscopy, and scanning electron microscopy with the capability to measure semiquantitative elemental compositions by energy-dispersive x-ray emission spectroscopy. Results indicate the presence of Tc metal on all samples as the primary electrodeposited constituent for all deposition times and Tc concentrations. Thin films of Tc have been observed followed by the formation of beads that are removable by scratching. After 2000, the quantity of Tc removed from solution and deposited was $0.64 \text{ mg Tc per cm}^2$. The solution, after electrodeposition, showed characteristic absorbances near 500 nm corresponding to hydrolyzed Tc(IV) produced during deposition of Tc metal. No detectable Tc(IV) was deposited to the cathode.
© 2011 The Electrochemical Society. [DOI: 10.1149/1.3533364] All rights reserved.

Manuscript submitted July 6, 2010; revised manuscript received December 9, 2010. Published xx xx, xxxx.

Technetium, element 43, has 34 radioactive isotopes that are known, with none being stable, from mass 85–118. The most common isotope, ^{99}Tc ($t_{1/2} = 2.14 \times 10^5 \text{ y}$), is present in large quantities in spent nuclear fuel, where it constitutes approximately 6% of the fission yield.¹ With regard to nuclear waste management, Tc presents a threat to the biosphere because it is very stable and mobile as the anion pertechnetate. Two methods to reduce the potential long-term environmental hazards of Tc have been considered: transmutation of Tc metal targets by neutron capture in a reactor to produce stable isotopes of ruthenium or the incorporation of Tc into stable forms for long-term geological disposal (i.e., Tc alloys or oxide materials).^{2,3} For this reason, the production of Tc metal for eventual use in a target or waste form represents a challenge for the management of nuclear wastes. Different methods to produce Tc metal have been reported.⁴⁻⁸ A common route of reduction is to use H_2 gas or an Ar/ H_2 mixture at $400\text{--}1100^\circ\text{C}$ from NH_4TcO_4 and TcO_2 .⁹ Secondary techniques such as the electrodeposition of Tc from aqueous solutions have also been previously explored as an option for the recovery of Tc as the metal. With regard to Tc electrodeposition, technetium is unique. It is a very complex element to study electrochemically because of its large variety of chemical forms, oxidation states, and known disproportion reactions available to it in various aqueous systems that have the ability to hinder production of Tc metal on a cathode substrate.⁹⁻¹² The potential uses of the electrodeposition of TcO_4^- for the recovery of Tc metal from aqueous solutions has gained notoriety as a possible method for the isolation of this fission product prior to being introduced into a waste form. This technique potentially eases the recovery of Tc from spent nuclear fuel and reprocessing activities. This may be used as a possible precursory step in the production of Tc metal, Tc containing waste forms, or thin films of Tc metal for target preparation. Attempts to electrodeposit Tc metal are often hindered due to the formation of oxides.^{13,14} Habitually, results are misleading or repeated experiments do not mimic results reported in literature. Because of this ambiguity, and because deposition products are not well structurally characterized, we have investigated the most simple system of TcO_4^- in H_2SO_4 , electrodeposited onto gold. In the current study, we report the main electrodeposition product of TcO_4^- in the presence of $1 \text{ M H}_2\text{SO}_4$ onto a gold foil cathode at current densities of 1 A/cm^2 as hexagonal Tc metal.

Experimental

Chemicals.— The starting material NH_4TcO_4 was obtained from stocks at the Los Alamos National Laboratory originally purchased from the Oak Ridge Office of Isotope Sales. Prior to use, the NH_4TcO_4 was purified by dissolution into a dilute $\text{NH}_4\text{OH}/\text{H}_2\text{O}_2$ solution followed by evaporation to dryness. The solutions used for electrodeposition were prepared by dissolving the dry NH_4TcO_4 into deionized (DI) water. The final concentration of the stock Tc solution was quantified by LS counting. Concentrated sulfuric acid was purchased from J.T.Baker and used as received. Gold foil, 0.1 mm thick 99.99% was purchased as a $25 \times 25 \text{ mm}$ sheet and cut into individual electrodes. Samples to be electrodeposited consisted of 10 mL stock solutions containing $[\text{H}_2\text{SO}_4] = 1 \text{ M}$ and $[\text{Tc}] = [2 \times 10^{-3}]$ and $[1 \times 10^{-2}] \text{ M}$ Tc representing 2 or 10 mg dissolved Tc. Additionally, solutions were not purged of oxygen, nor actively deaerated during deposition experiments. Crystalline TcO_2 was prepared by thermal decomposition of NH_4TcO_4 at 700°C under argon atmosphere whereupon the sample was collected for future use or was converted to Tc metal under $5\% \text{ H}_2/\text{Ar}$ atmosphere for an additional 24 h . Water was purified to $>18 \text{ M}\Omega \text{ cm}$ by a Milli-Q system. All other commercially available chemicals were used as received.

Experimental setup.— A three-electrode commercially available computer-controlled potentiostat (CH Instruments Electrochemical Workstation) was used for all Tc electrodeposition experiments. Solutions were rapidly stirred, without purging, at room temperature throughout the deposition with a constant current density of 1 A/cm^2 . Depositions were monitored against a $3 \text{ M Cl}^- \text{ Ag}/\text{AgCl}$ reference electrode. A solid sheet of platinum metal was used as the counter electrode with an exposed surface area of 2 cm^2 separated by 3 cm from the gold foil cathode. The gold foil was cut into sheets with an exposed deposition area of 0.25 cm^2 where the Tc was deposited. Following Tc deposition, electrodes were washed with DI water and allowed to air dry. Electrodes were prepared for x-ray diffraction (XRD), extended x-ray absorption fine structure (EXAFS), and scanning electron microscopy/energy-dispersive x-ray emission spectroscopy (SEM/EDS) analysis. The quantity of Tc deposited onto the gold foil was quantified by liquid scintillation counting (LSC). Following electrodeposition, the solutions were analyzed by UV-visible spectroscopy (Cary 6000i).

X-ray diffraction.— Electrodeposited Tc was examined by placing the portion of the electrode containing a Tc deposit directly onto a silicon wafer and held in place with moldable clay underneath the electrode. The XRD patterns were obtained using a Philips Panalyti-

² E-mail: mausolfe@unlv.nevada.edu

106 cal X'Pert Pro, Cu K α target with Ni filter and an X'elerator mul-
 107 tiple Si-strip solid-state detector. The XRD patterns were quantified
 108 by Rietveld analysis using the TOPAS 3.0 software.

109 *X-ray absorption fine structure spectroscopy.*— X-ray absorption
 110 fine structure (XAFS) measurements were completed at the Ad-
 111 vanced Photon Source (APS) at the BESSRC-CAT 12 BM station at
 112 Argonne National Laboratory. Technetium compounds (NH₄TcO₄,
 113 TcO₂, Tc metal, and deposited Tc) were diluted (~1% Tc in mass)
 114 in boron nitride or directly taped to the aluminum sample holders
 115 with kapton. XAFS spectra were recorded at the Tc–K edge
 116 (21,044 eV) in fluorescence mode at room temperature using a 13-
 117 element germanium detector. A double crystal of Si [111] was used
 118 as a monochromator for the photon source. The energy was cali-
 119 brated using steam-reformed Tc metal, decomposed from NH₄TcO₄,
 120 according to Ref. 16.

121 For each sample, four spectra were recorded in the k range (k
 122 = [0,17] Å⁻¹) and averaged. Background contribution was removed
 123 using ATHENA¹⁷ software and data analysis was performed using
 124 WINXAS.¹⁸ For the fitting procedure, amplitude and phase shift func-
 125 tions were calculated by FEFF8.2.¹⁹ Input files were generated by
 126 Atoms²⁰ using crystallographic structures of technetium dioxide.²¹
 127 Adjustments of the k^3 -weighted EXAFS spectra were performed un-
 128 der the constraints $S_0^2 = 0.9$. A single value of energy shift (ΔE_0)
 129 was used for all scattering. The uncertainty determined by EXAFS
 130 on the coordination number (CN) was $\pm 20\%$ and ± 0.02 Å on the
 131 reported atomic distances (R).

132 *Scanning electron microscopy and energy-dispersive X-ray emis-*
 133 *sion spectroscopy.*— SEM and EDS analysis were completed di-
 134 rectly on the electrodeposited samples. The SEM images and EDS
 135 measurements were performed using a JEOL-5610 scanning elec-
 136 tron microscope equipped with secondary electron and backscat-
 137 tered electron detectors with the capability to measure elemental
 138 analysis semiquantitatively by energy-dispersive x-ray emission
 139 spectroscopy.

140 *Other techniques.*— ⁹⁹Tc concentrations were evaluated by LS
 142 counting using a Packard 2500 scintillation analyzer. The scintilla-
 143 tion cocktail used was Ultima Gold AB (Packard). The concentra-
 144 tions of solutions prior to and following electrodeposition were de-
 145 termined using calibration curves performed in solution with a
 146 composition similar to the experimental parameters. All recorded
 147 UV-visible spectra were collected at room temperature in a 1 cm
 148 quartz cell on a Cary 6000i double beam spectrometer with back-
 149 ground subtraction.

150 Results

151 *X-ray powder diffraction.*— XRD patterns were recorded be-
 152 tween $2\theta = 20^\circ$ and $2\theta = 120^\circ$ with a step rate of 1.16°/min using
 153 the Bragg-Brentano method. The fitted patterns presented in Fig. 1
 154 confirm the formation of Tc metal with lattice parameters of $a(\text{Å})$
 155 = 2.74354(15) and $c(\text{Å}) = 4.39524(14)$ for 0.01 M Tc and $a(\text{Å})$
 156 = 2.74427(94) and $c(\text{Å}) = 4.4212(17)$ for 0.01 and 0.002 M Tc so-
 157 lutions electrodeposited for 500 s. These values are in agreement
 158 with literature.²²⁻²⁵ Tc metal has two crystalline phases, hexagonal
 159 and cubic. The cubic phase is produced at temperatures above
 160 800°C from the hexagonal phase. Lattice parameters are in agree-
 161 ment with the hexagonal phase; no other phases were detectable
 162 other than the gold foil that the deposit was adhering to. Though
 163 XRD is a useful tool to probe for the presence of Tc metal, the
 164 presence of amorphous, or other nondiffracting phases in a deposit
 165 cannot be completely distinguished from the diffracting metal de-
 166 posits on the electrode. Therefore, the need to provide more struc-
 167 tural information on the electrodeposited Tc was completed by
 168 XANES and XAFS spectroscopy.

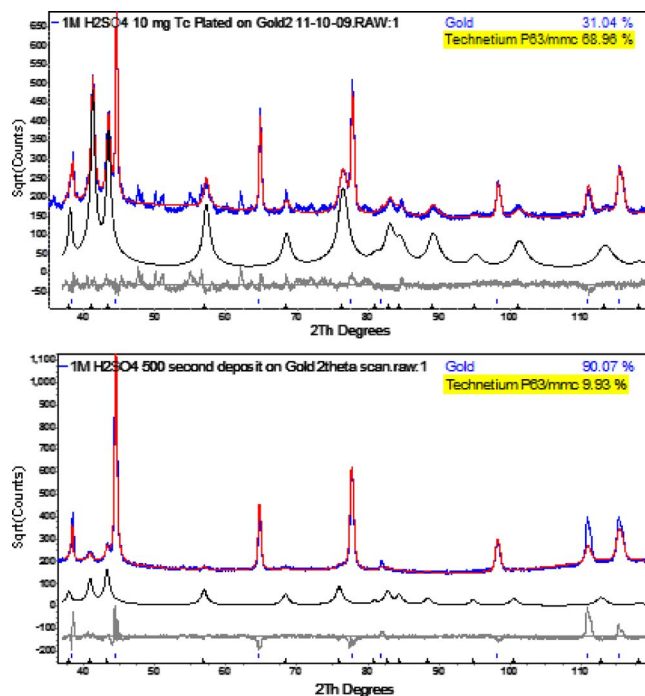


Figure 1. (Color online) XRD hexagonal Tc metal, [Tc] = 0.01 (top) and 2×10^{-3} M (bottom), [H₂SO₄] = 1 M, $t = 500$ s deposition.

169 XANES.— XANES provides local geometry of the electrodepos-
 170 ited sample. Three standards were used to provide spectra for Tc in
 171 the 0, IV, and VII oxidation states: Tc metal, TcO₂, and NH₄TcO₄.
 172 Figure 2 shows the absorption regions of each standard and one
 173 electrodeposited sample of Tc on the substrate from aqueous sulfuric
 174 acid solutions. All electrodeposited samples tested show similar re-
 175 sults in the XANES region for the shift in energy. The electrodepos-
 176 ited sample is Tc metal with the sample's shift in energy correspond-
 177 ing to that of the Tc metal standard. Additionally, there is no pre-
 178 edge peak in the XANES spectra further indicating that the
 179 originating Tc(VII) species is no longer present on the cathode after
 180 electrodeposition.

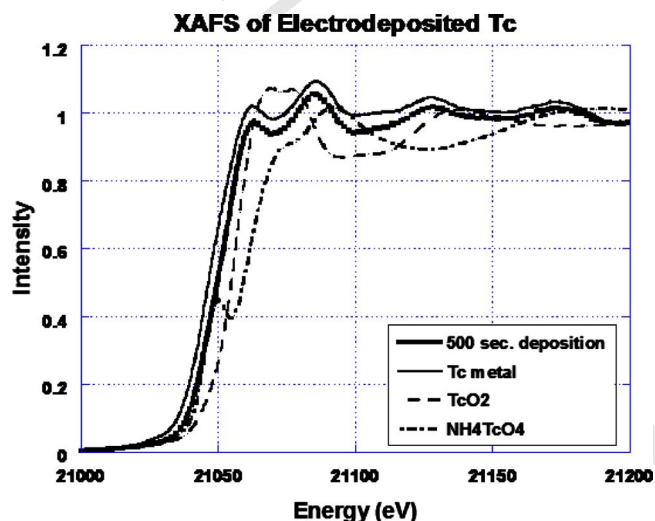


Figure 2. (Color online) XANES spectra of Tc₀, Tc(IV), and Tc(VII) and electrodeposited Tc, [Tc] = 0.01 M.

Table I. EXAFS structural parameters of electrodeposited Tc on gold; $[Tc] = 0.002$ M, $[H_2SO_4] = 1$ M, 500 s deposition, 1.0 A/cm². MS = multiscattering between the absorbing atom and neighboring Tc atom. CN = coordination number, R = radius, and σ^2 = Debye-Waller factor.

Tc	Structural Parameters		
Scattering Atom	C.N	R (Å)	σ^2 (Å ²)
Tc0-Tc1	5(1)	2.71(2)	0.007
Tc0-Tc2	5(1)	2.74(2)	0.006
Tc0-Tc3	5(1)	3.88(4)	0.008
Tc0-Tc4	15(3)	4.76(5)	0.009
MS (Tc0 and Tc2)	24	5.38(5)	0.015
MS (Tc2 and Tc5)	12	5.42(5)	0.02
Tc0-Tc5	6	5.42(5)	0.02
Tc0-Tc6	12	6.11(6)	0.015

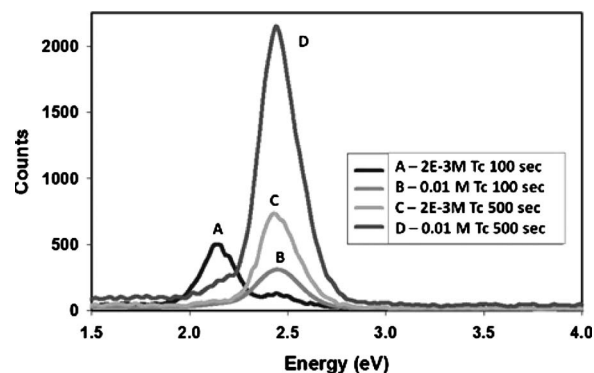


Figure 4. Electron dispersive spectra of electrodeposited Tc on gold, $t = 100$ and 500 s, $[H_2SO_4] = 1$ M, $[Tc] = 0.01$ and 2×10^{-3} M.

181 EXAFS.— In order to confirm the formation of Tc metal after
182 electrodeposition, XAFS measurements were performed on various
183 deposits of Tc. Results indicate that there is no Tc–O scattering and
184 no oxygen contribution in the Fourier transform corresponding to a
185 Tc–O peak. Table I shows the structural and scattering parameters
186 for the electrodeposited Tc and coordination distances. From $[Tc]$
187 = 0.01 M, the Tc₀–Tc₁ contribution has come from Tc–Tc, further
188 indicating the formation of hexagonal Tc metal after
189 electrodeposition.²⁶ Tc₀–Tc₂ scattering distance has been recorded
190 as 2.74(2) Å, further indicating the formation of hexagonal Tc metal
191 after electrodeposition from aqueous solution in 1 M H₂SO₄
192 (Fig. 3).

AQ: #4
193 Scanning electron microscopy and electron dispersive spectroscopy.
194 copy.— The cathode deposit obtained from the ammonium pertechnetate,
195 sulfuric acid solution appeared to be Tc metal. The deposit
196 was not dissolved by concentrated HCl and could be removed from
197 the cathode surface by scratching. The formation of a mirrored sur-
198 face is visualized immediately following electrodeposition of Tc for
199 all samples, across all deposition times and concentrations of Tc on
200 gold. The mirrored deposit on the electrode surface is possibly due
201 to the formation of a homogenous monolayer initially. This becomes

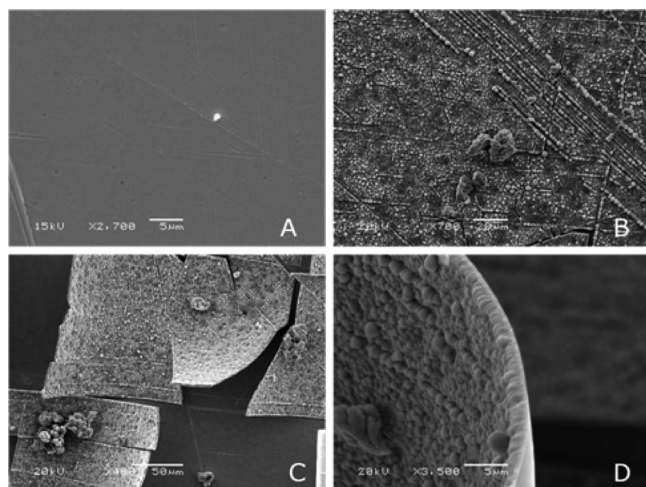


Figure 3. SEM micrographs for (A) formation of thin-layered Tc, $t = 100$ s deposition $[Tc] = 2 \times 10^{-3}$ M, $[H_2SO_4] = 1$ M; (B) formation of Tc beads, $t = 500$ s deposition, $[Tc] = 0.01$ M, $[H_2SO_4] = 1$ M; (C) mechanically stressed deposit layers of electrodeposited Tc (bright phase), gold foil underneath (dark phase), 500 s deposition with flake formation, $[Tc] = 0.01$ M, $[H_2SO_4] = 1$ M; and (D) initial Tc electrodeposited layer (250–750 nm) followed by bead formation and a new layer of Tc (1–3 μ m).

more dull following longer deposition times when the order of the
deposits becomes more randomized. The smooth, thin and lustrous
layer of Tc (Fig. 4a) formed on the gold foil has little texture which
forms layers of approximately 250–750 nm in thickness, as estimated
from Fig. 4d. A longer electrodeposition time was required to
form beads when deposited from less concentrated solutions. These
beads varied in diameter from 1 to 10 μ m, which formed on the
smooth mirrored surface (Fig. 4b). SEM indicated that the estimated
depth of the final layer is 1–3 μ m in thickness (Figs. 4c and 4d),
which does not significantly increase with longer deposition times.
Indication of this effect is observed by quantifying the electrodeposited
Tc from solution by LS counting before and after deposition of
the 0.01 M Tc solution.

The Tc absorption line corresponding to the K α 1 peak at 2.424 eV was monitored by EDS. EDS has shown the presence of Tc on the surface of the electrodeposited film from both 100 and 500 s deposition times in 1 M H₂SO₄ from solutions containing $[Tc] = 0.01$ and 2×10^{-3} M. The peaks corresponding to gold absorption lines at 2.123 eV were observed significantly for only one sample: the sample deposited from $[Tc] = 2 \times 10^{-3}$ M with a deposition time of 100 s. No significant peaks were observed for oxygen at 0.525 eV in any of the samples analyzed, though low energy oxygen x-rays are not readily detected by EDS. This helps further confirm the presence of Tc metal as the major constituent deposited in this electrodeposited series. The EDS Tc peak has also shown an increase in counts with an increase in deposition times and more concentrated.

LS counting.— LS counting was used to monitor the quantity of Tc remaining in solution after deposition. Quantities of deposit were estimated by this technique. For an electrodeposited sample initially containing 2 mg Tc in solution, after 2000 s of deposition, 0.167 mg of Tc metal was deposited with the highest rate of deposition occurring within the first 165 s (Fig. 5) with a final deposit of 0.64 mg Tc metal deposited per cm².

UV-visible (UV-vis) spectroscopy.— A slight change in the color of the solution was observed following deposition of Tc in all solutions. Following electrodeposition, both solutions with initial Tc concentrations of $[Tc] = 0.01$ and 0.002 M and constant sulfuric acid changed from translucent to slightly brown, as reported previously.²⁷ The $[Tc] = 0.01$ M solution, after electrodeposition, has a characteristic absorbance (Fig. 6) at 500 nm corresponding to a Tc(IV) species which formed during electrodeposition.

Conclusion

The present study has shown the ability to electrodeposit Tc metal onto gold foil cathodes. Results indicate that the morphology of the electrodeposited Tc from 1 M sulfuric acid solutions with high current produces Tc metal. The final Tc deposits were con-

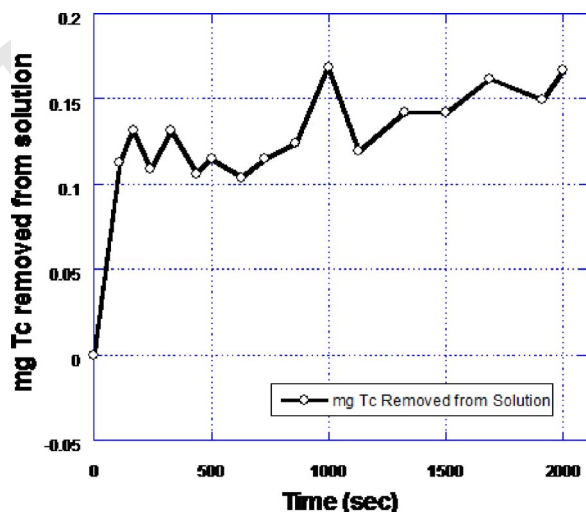


Figure 5. (Color online) LS counting of electrodeposited Tc onto gold foil; initially 2 mg Tc, 2000 s deposition, current density 1.0 A/cm², maximum Tc deposition 0.167 mg; 0.64 mg Tc/cm².

249 firmed as hexagonal Tc metal by powder XRD and XAFS with the
 250 latter indicating the absence of oxygen in the deposits. SEM/EDS
 251 has also confirmed the absence of oxygen in the deposits with a
 252 changing surface upon longer deposition times and higher concen-
 253 trations of Tc present during electrodeposition. UV-vis has indicated
 254 that the formation of Tc metal is hindered due to the formation of
 255 Tc(IV) species during electrodeposition. Further investigation into a
 256 range of solution conditions, various initial forms of Tc, and differ-
 257 ent types of cathodes are of interest in regard to future studies to
 258 understand the range of conditions that Tc metal can be electrode-

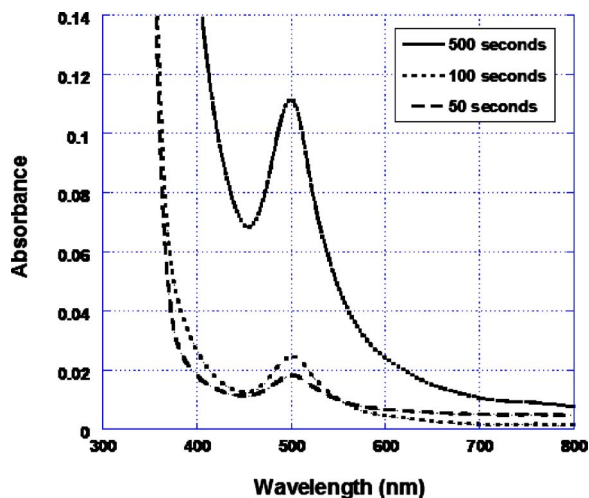


Figure 6. (Color online) UV-vis spectra of solution after electrodeposition, [Tc] = 0.01 M initially.

259 posited from. This work also presents an opportunity to use this as a
 260 recovery process for Tc metal prior to inclusion into a metallic waste
 261 form and an important possible option for management of Tc in
 262 nuclear waste streams.

Acknowledgment 263

The authors thank Tom O'Dou for outstanding health physics 264
 support and Dr. Gordon Jarvinen (Los Alamos) for a generous loan 265
 of ammonium pertechnetate. Funding for this research was provided 266
 by a subcontract through Battelle 0089445 from the U.S. Depart- 267
 ment of Energy, agreement No. DE-AC07-05ID14517. Use of the 268
 Advanced Photon Source was supported by the U.S. Department of 269
 Energy, Office of Science, Office of Basic Energy Sciences, under 270
 Contract no. DE-AC02-06CH11357. 271

University of Nevada assisted in meeting the publication costs of this 272
 article. 273

References 274

275
 1. K. Schwochau, *Technetium: Chemistry and Radiopharmaceutical Application*,
 Weinheim, Germany (2000). 276
 2. J. M. Bonnerot, V. Broudic, M. Phelip, C. Jegou, F. Varaine, X. Deschanel, M. F.
 Arnoux, and J. L. Faugere, *J. Nucl. Radiochem. Sci.*, **6**, 287 (2005). 277
 3. S. M. Frank, D. D. Keiser, and K. C. Marsden, in *Global 2007: Advanced Nuclear*
Fuel Cycles and Systems Proceedings, American Nuclear Society, La Grande Park,
 IL, pp. 1404–1411 (2007). 278
 4. J. W. Cobble, C. M. Nelson, G. W. Parker, W. T. Smith, and G. E. Boyd, *J. Am.*
Chem. Soc., **74**, 1852 (1952). 279
 5. S. Fried, *J. Am. Chem. Soc.*, **70**, 442 (1948). 280
 6. O. Muller, W. B. White, and R. Roy, *J. Inorg. Nucl. Chem.*, **26**, 2075 (1964). 281
 7. V. F. Peretrukhin, S. I. Rovnyi, V. V. Ershov, K. E. German, and A. A. Kozar, *Russ.*
J. Inorg. Chem., **47**, 637 (2002). 282
 8. V. I. Spitsyn, A. F. Kuzina, A. F. Tsarenko, A. A. Oblova, O. A. Balakhovskii, P. N.
 Kodochigov, M. P. Glazunov, and I. V. Kaimin, *Radiokhimiya*, **12**, 617 (1970). 283
 9. O. Courson, C. Le Naour, F. David, A. Bolyos, A. Maslennikov, and N. Papa-
 dopoulos, *Czech. J. Phys.*, **49/S1**, 687 (1999). 284
 10. W. D. Box, *Nucl. Appl.*, 155 (1985). 285
 11. B. L. Lawson, S. M. Scheifers, and T. C. Pinkerton, *J. Electroanal. Chem.*, **177**,
 167 (1984). 286
 12. J. D. Eakins and D. G. Humphries, *J. Inorg. Nucl. Chem.*, **25**, 737 (1963). 287
 13. A. Maslennikov, M. Masson, V. Peretroukhine, and M. Lecomte, *Radiochim. Acta*,
84, 53 (1999). 288
 14. A. Maslennikov, M. Masson, V. Peretroukhine, and M. Lecomte, *Radiochim. Acta*,
83, 31 (1998). 289
 15. TOPAS Version 2.0.: Profile and Structure Analysis Software for Powder Diffraction
 Data. User Manual; Bruker AXS: Karlsruhe, Germany (2000). 290
 16. F. Poineau, T. Hartmann, D. Jarvinen, and K. Czerwinski, *J. Radioanal. Nucl.*
Chem., **279**, 43 (2009). 291
 17. M. Newville, P. Livins, Y. Yacoby, E. A. Stern, and J. J. Rehr, *Phys. Rev. B*, **47**,
 14126 (1993). 292
 18. T. Ressler, *J. Synchrotron Radiat.*, **5**, 118 (1998). 293
 19. J. J. Rehr and R. C. Albers, *Rev. Mod. Phys.*, **72**, 621 (2000). 294
 20. B. Ravel, *J. Synchrotron Radiat.*, **8**, 314 (2001). 295
 21. E. E. Rodriguez, F. Poineau, A. Llobet, A. P. Sattelberger, J. Bhattacharjee, U. V.
 Waghmare, T. Hartmann, and A. K. Cheetham, *J. Am. Chem. Soc.*, **129**, 10244
 (2007). 296
 22. D. J. Lam, J. B. Darby, J. W. Downey, and L. J. Norton, *Nature*, **192**, 744 (1961). 297
 23. V. M. Golyanov, L. A. Elesin, and M. N. Mikheeva, *Pis'ma Zh. Eksp. Teor. Fiz.*,
18, 569 (1973). 298
 24. I. V. Vinogradov, M. I. Konarev, L. L. Zaitsev, and S. V. Shepel'kov, *Russ. J.*
Inorg. Chem., **23**, 1158 (1978). 299
 25. J. Haeglund, A. Fernandez Guillermet, G. Grimvall, and M. Kaerling, *Phys. Rev. B*,
48, 11685 (1993). 300
 26. F. Poineau, J. Du Mazaubrun, D. Ford, and J. Fortner, Uranium/technetium separa-
 tion for the UREX process—synthesis and characterization of solid reprocessing
 forms, ■ (■). 301
 27. R. E. Voltz and M. L. Holt, *J. Electrochem. Soc.*, **114**, 128 (1967). 302
 28. V. I. Spitsyn, A. F. Kuzina, A. A. Oblova, M. I. Glinkina, and L. I. Stepovaya, *J.*
Radioanal. Chem., **30**, 561 (1976). 303
 304
 305
 306
 307
 308
 309
 310
 311
 312
 313
 314
 315
 316
 317
 318
 319
 320
 321
 322
 323
 324
 325

AQ:
 #6

AUTHOR QUERIES — 068103JES

- #1 AU: Please verify the definition of “LS”.
- #2 AU: Please verify if box is correct here, or should something be inserted in its place.
- #3 AU: Please define XANES.
- #4 AU: Please check our change to the sentence beginning “Table I...” to ensure your meaning has been preserved.
- #5 AU: All figures must be cited in text. Please check our insertion of Fig. 3 citation.
- #6 AU: Please supply year and any other information for Ref. 26.

PROOF COPY [JES-10-1462R1] 068103JES